

SUPPORTING INFORMATION

The Influence of Superhydrophobicity on the Bactericidal Efficiency of Black Silicon Surfaces

Denver P. Linklater^{†, ‡}, Saulius Juodkazis[‡], Sergey Rubanov[§] Elena P. Ivanova[†]

[†]*Faculty of Life and Social Sciences, Swinburne University of Technology, Hawthorn, VIC 3122, Australia,*

[‡]*Centre for Micro-Photonics and Industrial Research Institute Swinburne, Faculty of Science, Engineering and Technology, Swinburne University of Technology, Hawthorn, VIC, 3122, Australia*

[§]*Advanced Microscopy Facility, Bio21 Institute, University of Melbourne, 30 Flemington Rd, 3010, Victoria, Australia*

*correspondence should be addressed to Elena P. Ivanova: eivanova@swin.edu.au

Contents:

Figure S1. Fabrication and characterization of black silicon surfaces

Figure S2. XPS analysis

Table S2. Bacterial strains cell surface characterizations

Figure S3. Characterisation of EPS production using confocal laser scanning microscopy

Figure S4. Comparative characterisation of black silicon and dragonfly wing surfaces

Figure S5. FIB/SEM of *E.coli* on black silicon surfaces

Fabrication and characterization of black silicon surfaces

During the plasma etching of silicon, or other materials, using etchant gases SF₆ and O₂, the production of silicon-oxy-fluoride complexes (dust particles) is initiated. These ‘dust’ particles grow in size within the plasma glow and settle onto the wafer forming random ‘micromasks.’ The ‘sticking’ of dust particles to the wafer surface protects random areas from ion bombardment, resulting in irregular growth of nanopillar features¹⁻³. The fabrication of black silicon was first reported by Her et al.,⁴ in 1998, and since then has been widely investigated for its uses in solar cells, micro-electronic-mechanical systems and photonic devices⁵⁻⁷.

Black silicon (bSi) was fabricated using single side polished p-type 100 mm silicon wafers. The wafers were thoroughly cleaned with isopropanol and then dried under nitrogen flow to remove contaminants. They were then etched directly with a Samco RIE-101iPH inductively coupled plasma (ICP) assisted reactive ion etching tool using the following process parameters: etchant gases SF₆/O₂ with respective flow rates of 35/45 sccm, process pressure of 1 Pa, ICP power of 150 W, and RIE bias power of 15 W. Silicon wafers were etched for 15, 30 and 45 min to produce surface nanostructures of varying heights and spacing. It is understood that the fabrication of bSi is a random, self-masking process whereby pillars are seeded indiscriminately during the etch process. Throughout alternating rounds of etching and deposition, the spontaneous passivation mask was not efficiently removed therefore a simple 10 wt. % sulphuric acid solution and sonication for 10 minutes was used to remove the contaminative mask.

BSi surfaces were characterised using high-resolution scanning electron microscopy (SEM) using an EBL/SEM tool (Raith150 two, Raith GmBH) at 5 kV, using magnifications ranging between ×5K and ×75K. Image processing software, Image J and Gwyddion (version 2.46)

were used to obtain pillar characteristics, spatial distributions and degree of clustering (density/ μm^2). A colour threshold was applied to binary SEM images in order to segment features within the image. Features that fall within the colour thresholding range are ‘counted’ giving the number and area of features which can be directly correlated to the diameter of the nanopillar caps. Image J was also used to find local maxima within SEM images in order to number the pillars within a given area. Gwyddion was used to apply a Fast-Fourier Transform (FFT) to SEM images in order to retrieve the average pillar-pillar distance.

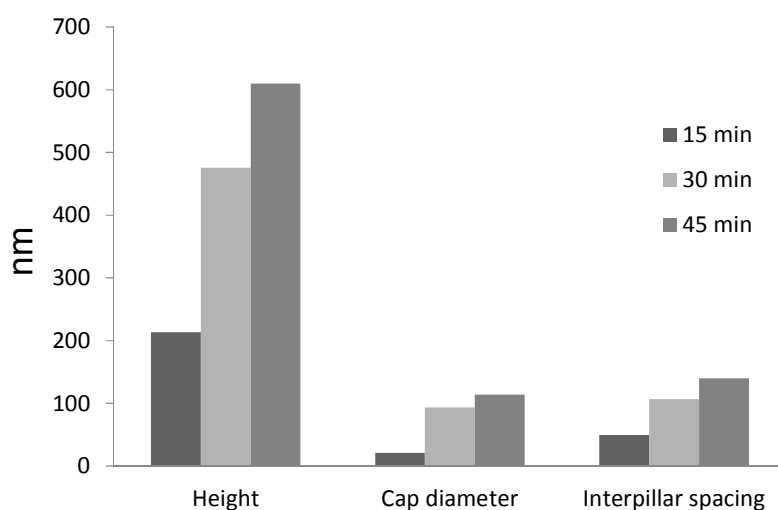


Figure S1. The time dependence of plasma etching of silicon wafers using SF_6 and O_2 etchants. A strong linear correlation is observed between etch time, height, cap diameter and spacing.

Wettability analysis

Static water contact angle measurements were performed on bSi samples using an FTA 1000c (First Ten Angstroms Inc.) which dispensed approximately $5.0 \mu\text{l}$ volume of water, by means of a nanodispenser tip, onto the substratum surface. Images were taken with a Pelco Model PCHM 575-4 camera within 1-2 sec of the drop being placed on the surface.

XPS analysis

XPS analysis was performed using a Thermo Scientific™ K-alpha X-ray Photoelectron Spectrometer (ThermoFischer), equipped with a monochromatic X-ray source (Al K α , $h\nu = 1486.6$ eV) operating at 150 W. The spectrometer energy scale was calibrated using the Au 4f $_{7/2}$ photoelectron peak at the binding energy (BE) of 83.98 eV. During analysis, the samples were flooded with low-energy electrons to counteract any surface charging that may take place. The hydrocarbon component of the C 1s peak (binding energy 284.8 eV) was used as a reference for charge correction. Photoelectrons emitted at 90° to the surface from an area of $700 \times 300 \mu\text{m}^2$ were analysed with 160 eV for survey spectra and then with 20 eV for region spectra. Survey spectra were recorded at 1.0 eV/step, while the region spectra were taken at 0.1 eV/step. The Shirley algorithm was used to measure the background core level spectra and chemically distinct species in the high-resolution regions of the spectra were resolved using synthetic Gaussian–Lorentzian components after the background was removed (using the Thermo Scientific™ Avantage Data System). The relative atomic concentration of elements determined using XPS was quantified on the basis of the peak area in the selected high-resolution region, with the appropriate sensitivity factors for the instrument being used. High resolution scans were performed across each of the carbon 1s, oxygen 1s, fluorine 1s, nitrogen 1s and silicon 2p $^{3/2}$ and 1/2 peaks.

Table S1. Atomic fractions of elements in percentage detected by XPS on the different bSi surfaces

Element	bSi	PFTS-bSi
C 1s	7.40 ± 0.96	28.83 ± 1.42
O 1s	49.47 ± 0.40	13.93 ± 0.68

Si 2p	42.67 ± 0.59	12.27 ± 0.45
N 1s	0.20 ± 0.01	0.20 ± 0.01
F 1s	0.20 ± 0.01	44.80 ± 0.70

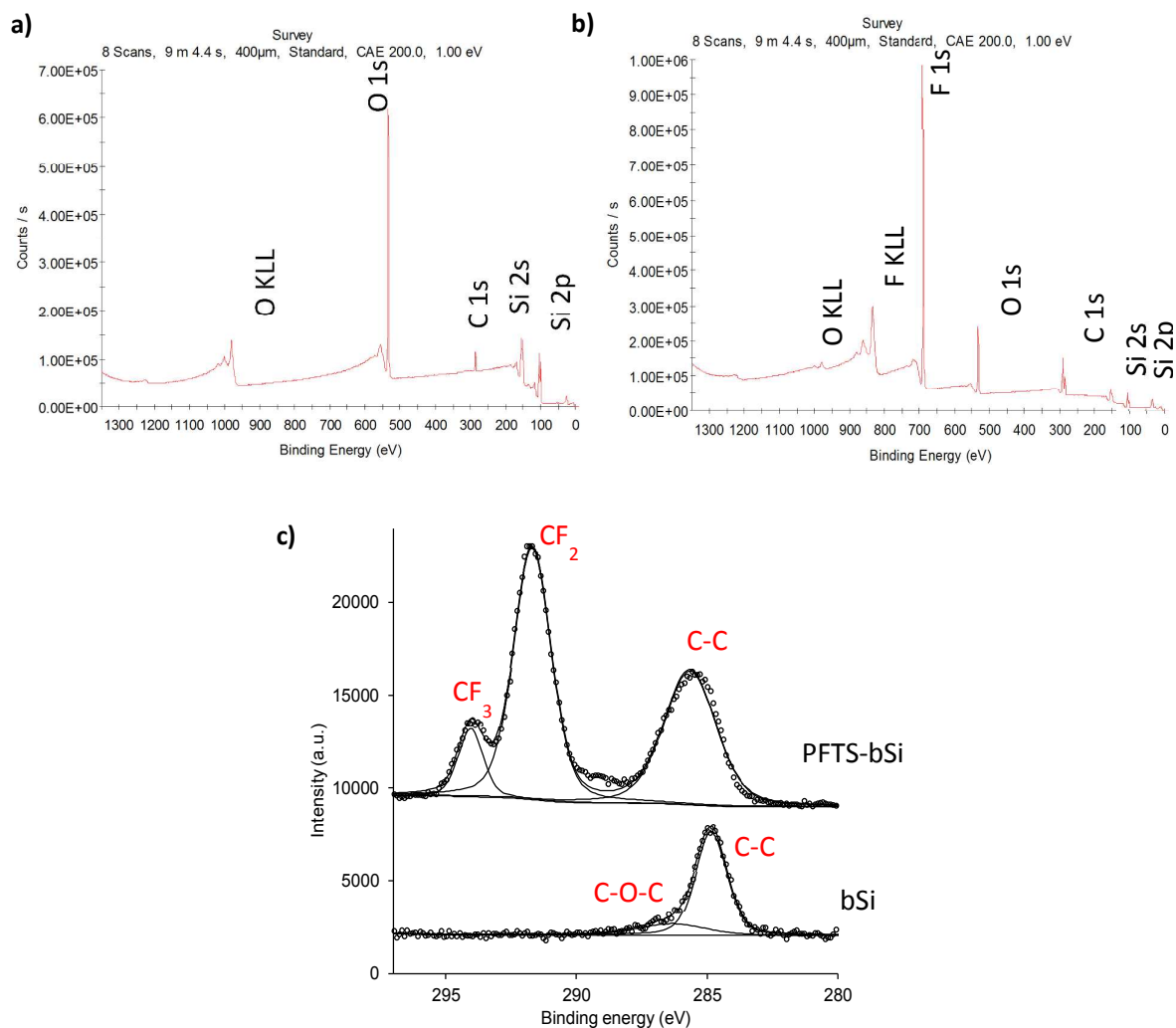


Figure S2. XPS survey spectra of (a) bSi surface and (b) PFTS coated bSi surface. (c) deconvoluted high resolution C spectra taken of the C-1s region of different bSi surfaces (adventitious carbon presents on control bSi). The bound layer of PFTS on bSi presents with carbon-fluorine bonding indicated by the C-F₃ and C-F₂ bonds found in PFTS.

Bacterial strains growth condition and cell surface characterizations

Pseudomonas aeruginosa ATCC 9721 and *Staphylococcus aureus* CIP 65.8^T, were obtained from American Type Culture Collection ATCC and Culture Institute Pasteur, France, respectively, and refreshed on nutrient agar (Oxoid) until the logarithmic phase of growth (24 h at 37° C). Bacterial cell suspensions of an optical density 0.1 (OD₆₀₀ = 0.1) were prepared by suspending 1 loopful of bacteria in 5 ml nutrient broth (Oxoid) and further diluting until the correct optical density was achieved using (Halo RB-10, Dynamica).

The physicochemical cell surface characteristics were determined in our previous work (Table S2)⁸ by measuring the cell surface wettability and charge. The surface wettability of *P. aeruginosa*, and *S. aureus* was evaluated from contact-angle measurements on lawns of bacterial cells using the sessile drop method in the FTA200 instrument. A bacterial cell suspension was prepared and applied to the glass substrata and measurements were performed. Bacterial surface charge was inferred via measurement of the electrophoretic mobility (EPM) of the bacterial cells, followed by conversion into a zeta potential using Smoluchowski's approximation. The EPM was measured as a function of ionic strength in a buffered solution using a zeta potential analyzer (ZetaPALS; Brookhaven Instruments Corp). The cell suspension was prepared and measurements were taken as explained elsewhere⁸. All measurements were carried out in triplicate, and for each sample, the final EPM represents the average of five successive ZetaPALS readings, each of which consisted of 14 cycles per run.

Table S2. Cell surface characteristics of *P. aeruginosa* and *S. aureus* ⁸

Strain	Water Contact angle (°)	EPM [(μ/s) (V/cm)]	Zeta potential, ζ (mV)
<i>P. aeruginosa</i> ATCC 9721	43.3 ± 8	-1.1 ± 0.1	-14.4 ± 0.7
<i>S. aureus</i> CIP 65.8	72.2 ± 8	-2.8 ± 0.8	-35.2 ± 1.0

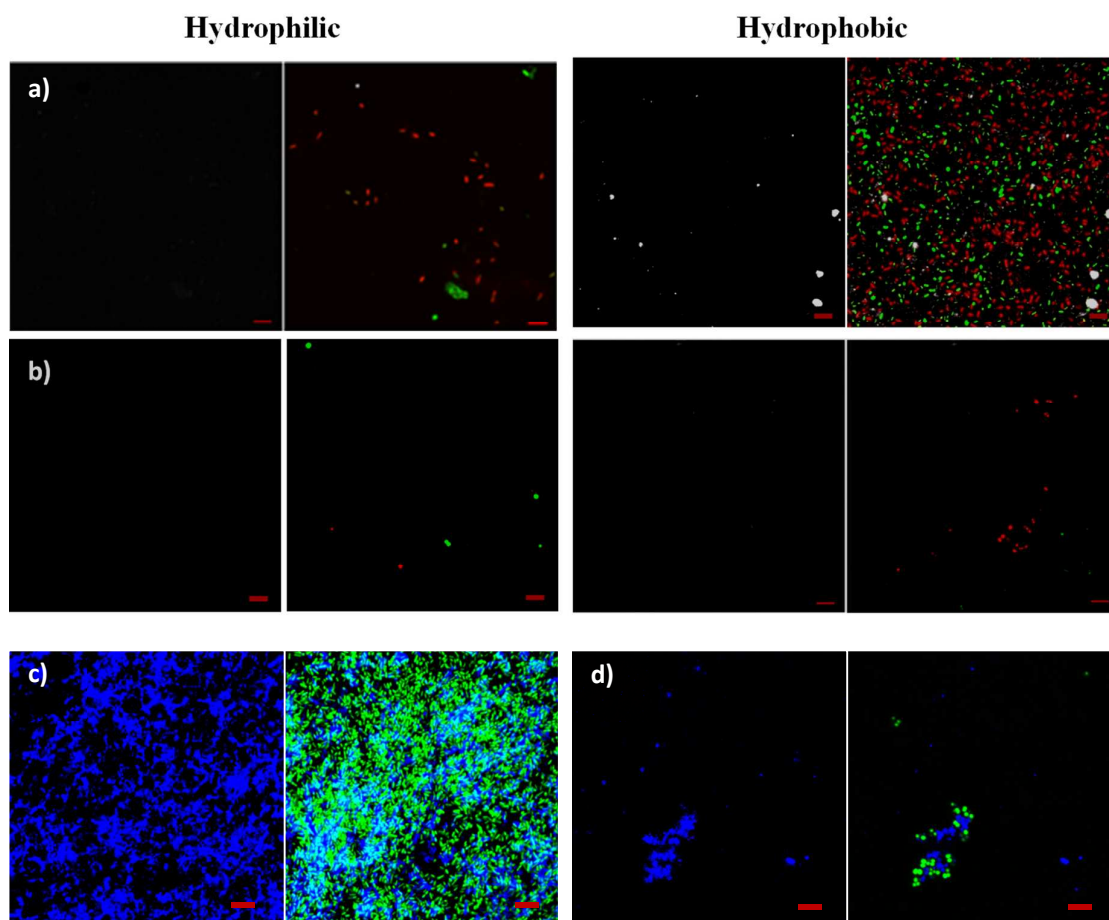


Figure S3. Staining of EPS with Alexa Fluor[®] Concanavalin A conjugate 633 and LIVE/DEAD Baclight (a) *P. aeruginosa* and (b) *S. aureus*, resulting in none or very little extracellular polysaccharides production despite large attachment numbers for *P. aeruginosa* on superhydrophobic surfaces (top-right cnr). Left image shows the single channel for excitation of Con A (shown in white) and second image shows the overlay with FITC and PI channels (red and green). Bottom images show control surfaces for (c) *P. aeruginosa* and (d) *S. aureus* revealing high amounts of EPS (shown in blue). Scale bars are 5 μm.

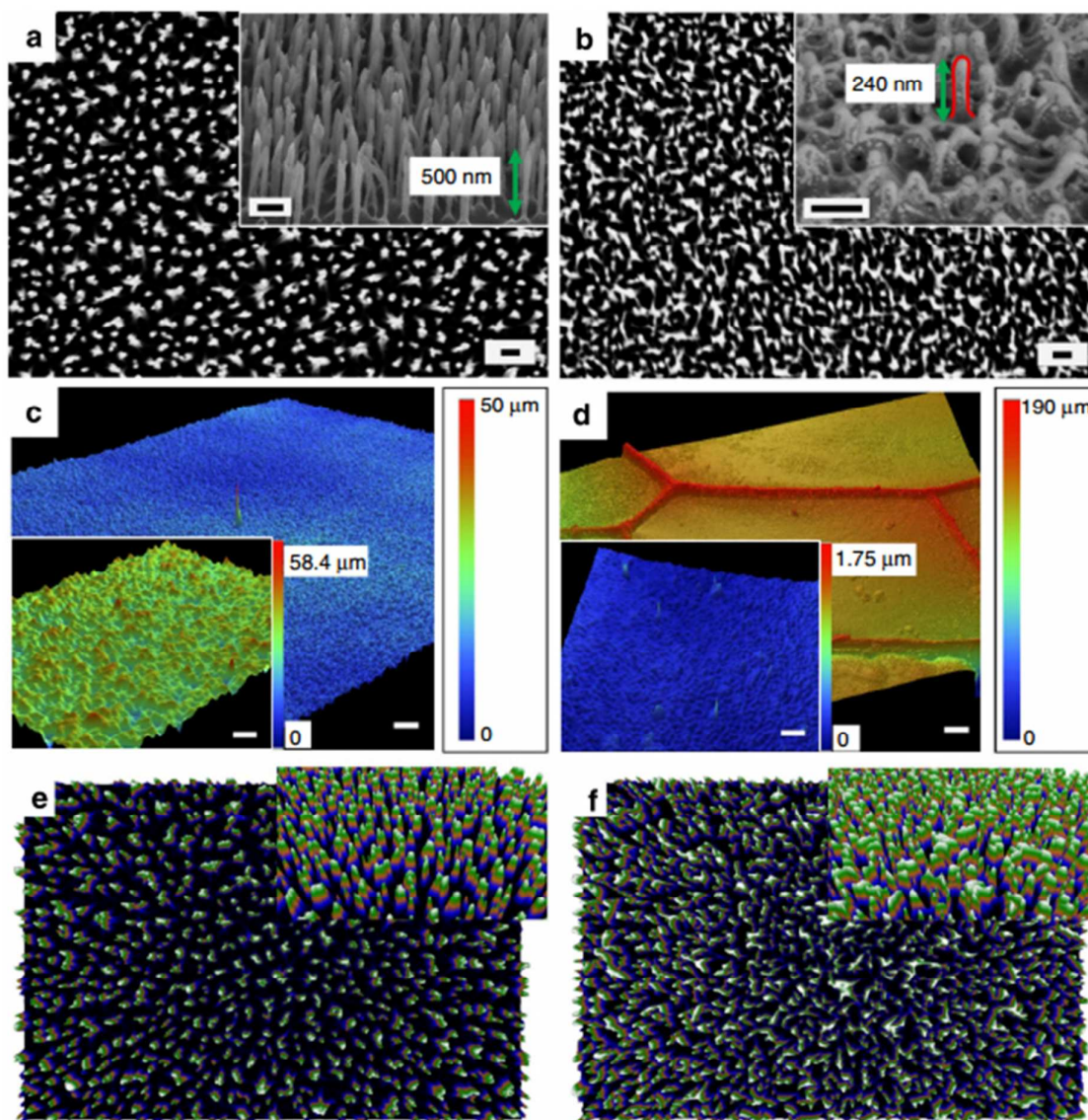


Figure S4. Characterization of black silicon and *D. bipunctata* wings according to our previous work⁹. Scanning electron micrographs of the upper surface of (a) bSi and (b) dragonfly forewings at $\times 35,000$ magnification demonstrate the surface patterns of the two samples. Scale bars, 200 nm. Micrographs tilted at an angle of 53 (inset) show sharper nanopillars of black silicon distinct from one another and approximately twice the height of those of the dragonfly wing. Optical profilometry shows the nanoprotusions of (c) bSi and (d) dragonfly forewings. Scale bars, 50 μm ; inset, 2 μm . Three-dimensional reconstructions based on a displacement map technique further highlight the differences and similarities of (e) bSi and (f) dragonfly forewings. Used with permission obtained from ref⁹. Copyright Nature Publishing Group 2013.

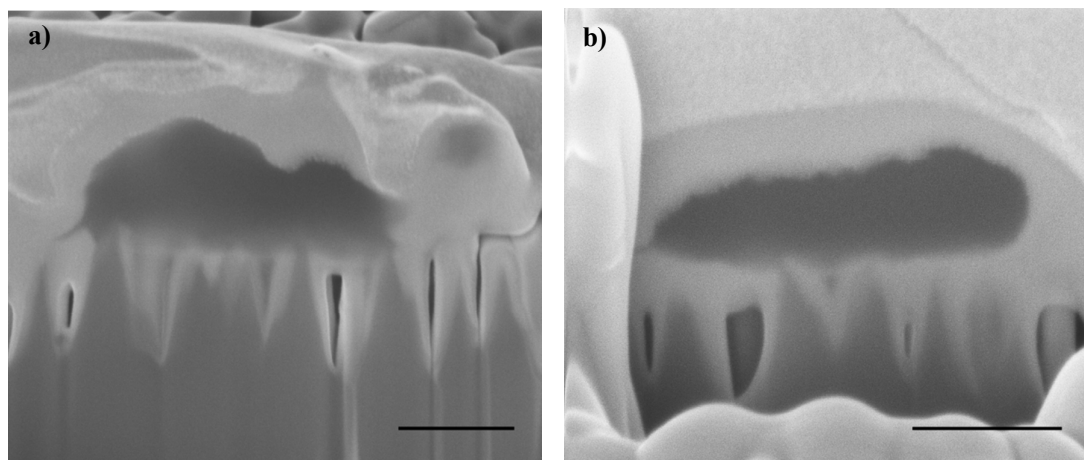


Figure S5. FIB milling of *E. coli* (K12) post 30 minutes' incubation on hydrophilic (a) and hydrophobic (b) bSi surfaces. The indentations made by the nanopillars as the *E. coli* cell settled onto the bSi surfaces are clearly seen in the SEM images. Scale bars are 400 nm.

References:

- (1) Jansen, H. V.; de Boer, M. J.; Unnikrishnan, S.; Louwerse, M. C.; Elwenspoek, M. C., Black Silicon Method: X. A Review on High Speed and Selective Plasma Etching of Silicon with Profile Control: An in-Depth Comparison between Bosch and Cryostat Drie Processes as a Roadmap to Next Generation Equipment. *J. Micromech. Microeng.* **2009**, *19* (3), 033001.
- (2) Jansen, H.; Boer, M. d.; Legtenberg, R.; Elwenspoek, M., The Black Silicon Method: A Universal Method for Determining the Parameter Setting of a Fluorine-Based Reactive Ion Etcher in Deep Silicon Trench Etching with Profile Control. *J. Micromech. Microeng.* **1995**, *5* (2), 115-120.
- (3) Jansen, H. V.; de Boer, M. J.; Ma, K.; Gironès, M.; Unnikrishnan, S.; Louwerse, M. C.; Elwenspoek, M. C., Black Silicon Method Xi: Oxygen Pulses in Sf 6 Plasma. *J. Micromech. Microeng.* **2010**, *20* (7), 075027.
- (4) Her, T.-H.; Finlay, R. J.; Wu, C.; Deliwala, S.; Mazur, E., Microstructuring of Silicon with Femtosecond Laser Pulses. *App. Phys. Lett.* **1998**, *73* (12), 1673-1675.
- (5) Bao, X.; Liu, F.; Zhou, X., Photovoltaic Properties of Black Silicon Microstructured by Femtosecond Pulsed Laser. *Optik* **2012**, *123* (16), 1474-1477.
- (6) Balcytis, A.; Ryu, M.; Seniutinas, G.; Nishijima, Y.; Hikima, Y.; Zamengo, M.; Petruškevičius, R.; Morikawa, J.; Juodkazis, S., Si-Based Infrared Optical Filters. *Optic. Eng.* **2015**, *54* (12), 127103.
- (7) Liu, X.; Coxon, P. R.; Peters, M.; Hoex, B.; Cole, J. M.; Fray, D. J., Black Silicon: Fabrication Methods, Properties and Solar Energy Applications. *Energy Environ. Sci.* **2014**, *7* (10), 3223-3263.
- (8) Mitik-Dineva, N.; Wang, J.; Truong, V. K.; Stoddart, P.; Malherbe, F.; Crawford, R. J.; Ivanova, E. P., Escherichia Coli, Pseudomonas Aeruginosa, and Staphylococcus Aureus

Attachment Patterns on Glass Surfaces with Nanoscale Roughness. *Curr. Microbiol.* **2008**, *58* (3), 268-273.

(9) Ivanova, E. P.; Hasan, J.; Webb, H. K.; Gervinskas, G.; Juodkazis, S.; Truong, V. K.; Wu, A. H. F.; Lamb, R. N.; Baulin, V. A.; Watson, G. S.; Watson, J. A.; Mainwaring, D. E.; Crawford, R. J., Bactericidal Activity of Black Silicon. *Nat. Commun.* **2013**, *4*.